

Reconstruction of 1852 Banda Arc megathrust earthquake and tsunami

TszMan L. Fisher¹ · Ron A. Harris¹

Received: 5 November 2015 / Accepted: 27 April 2016 / Published online: 6 May 2016
© Springer Science+Business Media Dordrecht 2016

Abstract In 1852, a 5-min long earthquake struck the Banda Arc region of Indonesia that was felt over most of Indonesia. It caused uplift of new islands and sent a tsunami across the Banda Sea that reached a height of 8 m at Banda Neira and was also registered at Ambon, Saparua and other islands. Records of the 1852 earthquake at multiple locations provide the constraints needed to reconstruct the disastrous event through numerical modeling using Clawpack. Tsunami heights at various locations are the primary observations we use to test modeling results. The best fit models indicate that the earthquake was most likely a megathrust event along the Tanimbar Trough of $>M_w$ 8.4. At least 10–15 m of elastic strain has accumulated along the Tanimbar Through since the 1852 event, which is enough to cause an earthquake of similar size to the one in 1852. However, 10 times more people in the region are exposed to tsunami hazards than in the past.

Keywords Megathrust earthquake · Tsunami modeling · Eastern Indonesia · Banda Arc · Tanimbar Trough · Historical earthquake

1 Introduction

The purpose of this paper is to reconstruct the 1852 eastern Indonesian earthquake and tsunami from historical accounts, numerical modeling and a site visit. This event was felt over a 2000 km wide area and created a wide-spread tsunami across the Banda Sea. Numerical models of geophysical events like these provide a way to determine the likely source region and fault parameters of the earthquake and to assess the impact a reoccurrence of this event will have on densely populated coastal communities. The population in coastal regions of eastern Indonesia has increased tenfold since 1852. During this time of

✉ TszMan L. Fisher
tszman.lau44@gmail.com

¹ Brigham Young University, Provo, UT, USA

rapid growth, there has not been a major earthquake or tsunami in the region. At convergence rates of 75–110 mm/year, up to 10–15 m of potential slip has likely accumulated along some plate boundary segments (Harris 2011; Harris and Major 2016).

Tsunami models of the 1852 event can inform coastal communities how to prevent tsunami hazards from becoming full-scale disasters by providing tsunami inundation estimates for densely populated coastal communities. One of the greatest lessons learned from the 2011 Tohoku Earthquake is the importance of incorporating historic records into hazard models. This devastating earthquake struck in areas designated as low probability in the seismic hazard models used at the time (Stein et al. 2012). The models were based mostly on instrumental records over the past 50–70 years versus geological and historical data. Megathrust earthquakes, such as the Tohoku event and several recent events in Indonesia, reoccur at intervals of hundreds to thousands of years. By factoring in historical earthquake records to probability estimates, Tohoku had one of the highest probabilities of a megathrust event (i.e., Kelleher et al. 1973). Geological records, such as tsunami deposits, also provided evidence that megathrust earthquakes had occurred offshore Tohoku (Minoura et al. 2001).

Wichmann (1918) compiled an invaluable record of historic earthquakes and tsunamis that struck the Indonesian region during most of the Dutch colonial period (1500–1877). However, this compilation, which was published during colonial times in old German and Dutch, has not been available until recently when it was translated into English (Harris and Major 2016). The catalog documents frequent megathrust earthquakes and tsunami in the region. Some of the major events that happened in the 1800's in western Indonesia have reoccurred in the last 10 years along similar patches of the subduction interface as reconstructed from the Wichmann catalog (Newcomb and McCann 1987).

Reconstructions of historic earthquake events in other parts of Indonesia are needed to more accurately assess the disaster potential of large earthquakes and tsunamis. Numerical models of some of these events are possible if both the arrival times after shaking and run-up heights of tsunamis they caused were recorded. These crucial data make it possible to reconstruct the likely source region of the event and its moment magnitude. This approach has proven useful for discovering previously unknown source regions of megathrust earthquakes in eastern Indonesia (Liu and Harris 2013). Some of the tsunamis are also recorded in the recent geologic record (Harris and Major 2016).

1.1 Tectonic setting

Indonesia is at the heart of a three-way tectonic collision between the Australian, Asian and Pacific Plates. It is located along the Southeast edge of continental SE Asia, which is the upper plate to two major subduction zones. The Sunda subduction system forms along the western and southern edge of Indonesia where the Australian plate is converging at a rate of 50–75 mm/year (Fig. 1; Nugroho et al. 2009). Along the eastern side of Indonesia is a series of subduction zones and transform faults that form the plate boundary with the Pacific Plate, which converges at a rate of 100–110 mm/year (Kreemer et al. 2000). The Banda Arc, where the lower plate includes parts of the northern Australian passive continental margin, connects the Sunda and eastern Indonesia subduction systems through a bend of 180° (Fig. 1).

The western part of the Sunda Arc has experienced several megathrust earthquakes over the past decade (Yeates 2012). However, the eastern part of the Sunda Arc, Banda Arc and eastern Indonesia subduction zones remained relatively quiet over the past 150 years (Harris and Major 2016). GPS measurements throughout the Banda Arc show that elastic

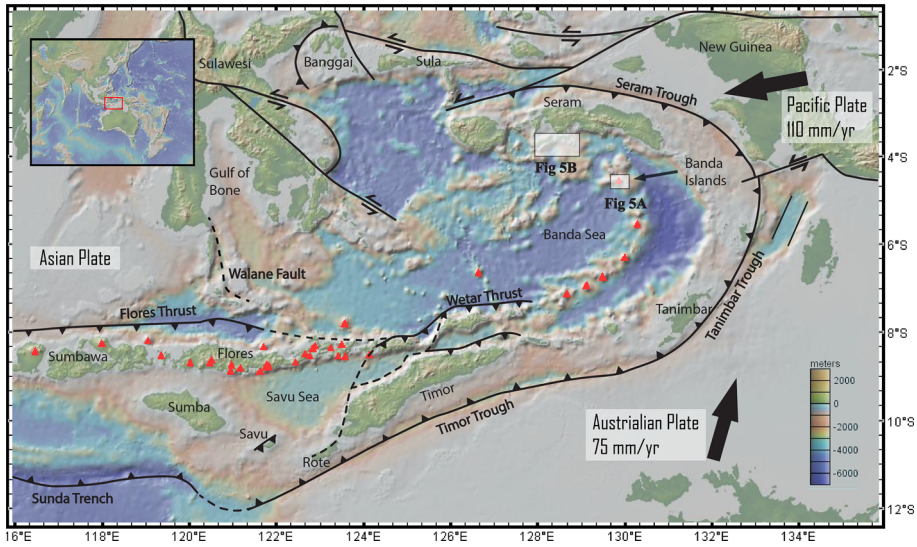


Fig. 1 Digital elevation model and tectonic features of Eastern Indonesia. Red triangles represent active volcanoes and black lines indicate major active faults along plate boundary segments. Plate motions are relative to the Asian Plate

strain is accumulating in a diffuse zone between the Timor Trough and Sulawesi (Nugroho et al. 2009). Within this zone are the Wetar and Flores backarc thrust systems (Fig. 1). The Wetar backarc thrust is accommodating up to 60 % of the plate convergence (Harris 1991, 2011). However, this thrust may not produce a long enough rupture for a megathrust event. The most likely active faults to generate a giant earthquake and regional tsunami are the Timor, Tanimbar and Seram Troughs of the Banda Arc-Continent Collision zone. At least 22 mm/year of convergence along these large plate boundary segments is loading in the Timor and Tanimbar Trough (Nugroho et al. 2009). The convergence rate on the Seram Trough is twice as fast (Rangin et al. 1999).

2 Historic earthquakes of eastern Indonesia

2.1 Wichmann catalog

Major geophysical events were recorded in Indonesia during the Dutch colonial era. These observations were later compiled and published as “The Earthquakes of the Indian Archipelago” by Arthur Wichmann (1918), known here as the Wichmann catalog. This catalog documents 166 destructive earthquakes and 43 tsunamis between 1538 and 1877 (Wichmann 1918). From 1600 to 1877, at least 600 major and minor earthquakes and 21 tsunamis were documented in the southern Banda Sea region alone, namely in the Banda Islands, Ambon, Haruku, Saparua, Seram and Timor (Fig. 2). The abundance of earthquakes in the region waxed and waned with peaks of activity during 1629–1644, 1675–1711, 1754–1775, 1815–1846, and 1850-to the end of the record (1877). The 1814–1846 cluster included the eruption of Tambora, which is Earth’s largest historic eruption (Harris and Major 2016). The earthquake clusters are bounded by major events at

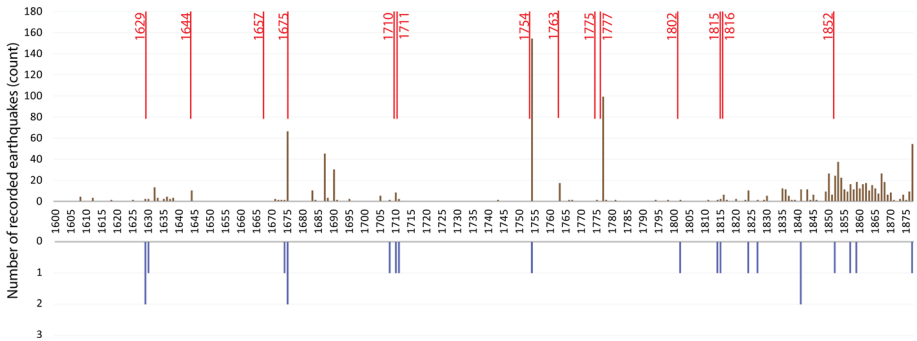


Fig. 2 Major historical earthquakes (red), number of all historical earthquakes (black) and number of tsunamis (blue) in Maluku Region from 1600 to 1877 in Wichmann catalog. Major earthquakes shake for >2 min, damage well-constructed buildings, are felt across the Banda Sea are followed by over 8 days of aftershocks

the beginning and ends of each period and have temporal distribution tails that diminish with time in the typical pattern of aftershocks. Major earthquake events with over 2 min of shaking commonly damaged well-constructed buildings (i.e., government buildings). These events were also felt across the region and were followed by weeks of aftershocks (Fig. 2). Most of these events were also accompanied by tsunamis.

From the first reliable account of earthquake damage in 1608, there have been at least 77 destructive earthquakes and 32 tsunamis in the southern Banda Sea region (Fig. 3; Table 1; Latief et al. 2000; BMKG 2011; Soloviev and Go 1984). During the 270-year period of the Wichmann catalog (1608–1877), there were 49 destructive earthquakes and 22 tsunamis. During the 136 years since this time (1878–2014), there have been 28 destructive earthquakes and 10 tsunamis (Latief et al. 2000). The rate of destructive earthquakes for both time periods is one major event every 5 years. The rate of destructive earthquakes associated with tsunamis is a bit higher in the earlier time period (1608–1877) than the later one (1878–2014), once in every 12 years versus once in every 14 years,

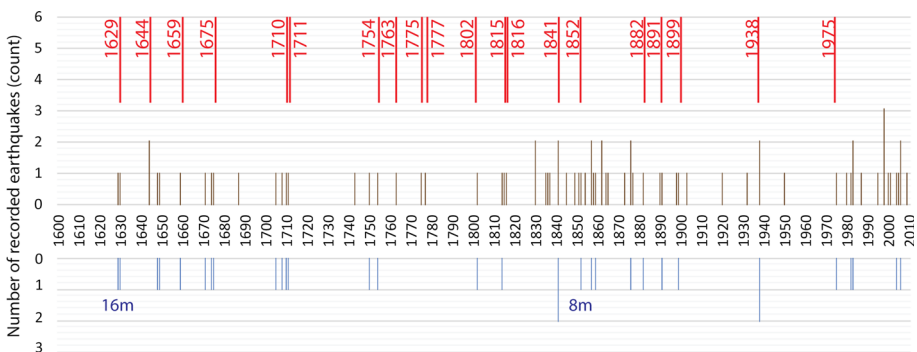


Fig. 3 Major earthquakes (red), number of destructive earthquakes (black), and number of destructive tsunamis (blue) in Maluku region from 1600 to 2014. Records are compiled from catalogs by Wichmann (1815), Latief et al. (2000); Soloviev and Go (1984) and BM. KG of Indonesia (2012). Blue numbers indicate the recorded run-up heights on Banda Islands in the 1629 and 1852 earthquakes

Table 1 List of destructive earthquakes and tsunamis from 1600 to 2014 in Maluku region (Wichmann 1918; Latief et al. 2000; Gempabumi 2011; Soloviev and Go 1984)

Year	Month	Day	Latitude	Longitude	Magnitude (Mo)	Depth (km)	Observed area	Source
1629	8	1	-	-	-	-	Ambon, Banda Islands	WM, LT, K
1630	-	-	-	-	-	-	Banda Islands	LT
1644	5	12	-	-	-	-	Ambon	WM
1644	5	17	-	-	-	-	Ambon, Haruku, Seram	WM
1648	2	29	-	-	-	-	Ambon	WM, LT, K
1649	-	-	-	-	-	-	Kei Islands	WM
1659	12	-	-	-	-	-	Ambon, Buru, others	WM, K
1671	10	17	-	-	-	-	Ambon, Haruku, Saparua	WM
1674	5	6	-	-	-	-	Ambon, Hitiu	LT
1675	2	17	-	-	-	-	Ambon, Uliassera	WM, LT, K
1687	2	19	-	-	-	-	Ambon	WM
1705	10	-	-	-	-	-	Ambon	WM
1708	11	28	-	-	-	-	Ambon	WM
1710	3	6	-	-	-	-	Banda Islands	WM, LT, K
1711	9	5	-	-	-	-	Ambon, Banda Islands, Haruku	WM, K
1743	-	-	-	-	-	-	Banda Islands	WM
1750	5	10	-	-	-	-	Banda Islands	WM
1754	8	18	-	-	-	-	Ambon, Uliassera	WM, K
1763	9	12	-	-	-	-	Banda Islands, Pulu Ai	WM, K
1775	4	19	-	-	-	-	Ambon	WM, K
1777	3	30	-	-	-	-	Ambon	WM, K
1802	8	25	-	-	-	-	Ambon, Banda Islands	WM, LT, K
1814	-	-	-	-	-	-	Banda Islands, Kiser	LT
1815	4	11	-	-	-	-	Ambon, Banda Islands	WM, K
1816	4	11	-	-	-	-	Banda	WM
1830	3	28	-	-	-	-	Ambon	GP

Table 1 continued

Year	Month	Day	Latitude	Longitude	Magnitude (Mo)	Depth (km)	Observed area	Source
1830	3	28	-	-	-	-	Ambon	WM, LT
1835	11	1	-	-	-	-	Ambon, Banda Islands, Saparua	WM, GP
1836	9	16	-	-	-	-	Ambon	WM
1837	1	21	-	-	-	-	Haruku, Nusalaut, Saparua	GP
1841	11	26	-	-	-	-	Banda Islands	LT
1841	12	16	-	-	-	-	Ambon	GP
1845	6	22	-	-	-	-	Ambon	WM
1849	5	28	-	-	-	-	Ambon, Saparua	WM
1851	11	20	-	-	-	-	Ambon, all	WM
1852	11	26	-	-	-	-	Banda Islands, Uiassera	WM, LT, K, GP
1854	12	-	-	-	-	-	Banda Islands	WM
1857	4	6	-	-	-	-	Banda Islands, Pulu Ai, Rosengain	WM
1857	5	13	-	-	-	-	Banda Sea, Timor, Dili	LT
1858	11	9	-	-	-	-	Ambon	LT, GP
1859	9	25	-	-	-	-	Banda Islands	LT
1862	9	15	-	-	-	-	Banda Islands	LT, GP
1862	10	15	-	-	-	-	Ambon; Banda Islands	WM
1864	9	14	-	-	-	-	Banda Islands	WM
1865	9	9	-	-	-	-	Banda Islands	WM
1873	11	4	-	-	-	-	Ambon, Seram	WM
1876	5	28	-	-	-	-	Ambon, Buru, Seram	WM, LT, GP
1876	7	12	-	-	-	-	Ambon	WM
1877	6	6	-	-	-	-	Banda Islands, Ambon	WM
1882	10	10	-	-	-	-	Banda Islands	K
1890	11	23	-	-	-	-	Banda Islands	LT, GP
1891	6	20	-	-	-	-	Ambon, Banda Islands, Saparua	K

Table 1 continued

Year	Month	Day	Latitude	Longitude	Magnitude (Mo)	Depth (km)	Observed area	Source
1898	1	17	-	-	-	-	Ambon	LT, GP
1899	9	30	-	-	-	-	Seram	K
1903	2	14	-	-	-	-	Banda Islands	LT, GP
1920	5	10	-	-	-	-	Ambon, Banda Islands, Saumlaki	LT, GP
1942	9	9	-3.5	128.3	-	-	Seram, Tolehubay	LT, GP
1938	2	1	-	-	-	-	Banda Islands, Banda Sea	LT
1938	2	2	-5	131.5	8.5	33	Banda Islands, Kei Islands	GP
1950	10	8	-	-	-	-	Ambon, Seram	K
1975	1	15	-5	130	5.9	<i>normal</i>	Banda Islands	LT, GP
1980	8	17	-3.77	128.24	5.4	24	Ambon	LT, GP
1982	3	12	-	-	-	-	Ambon	LT
1983	3	12	-4.06	127.92	6.9	17	Ambon, Seram	GP
1983	3	12	-4.04	127.89	5.8	33	Ambon	LT, GP
1987	7	17	-5.58	130.79	6.8	67	Ambon, Banda Islands	GP
1995	12	25	-6.903	129.151	7	142	Ambon, Saumlaki, Sorong	GP
1998	2	19	-4.476	129.082	6.5	33	Ambon	GP
1998	11	9	-6.954	129.022	6.5	33	Ambon, Darwin	GP
1998	11	9	-6.92	128.946	7	33	Ambon, Darwin	GP
2000	8	28	-4.11	127.394	6.6	16	Ambon	GP
2001	3	19	-4.03	128.02	6.5	33	Ambon	GP
2004	1	28	-3.01	127.44	6.8	33	Ambon, Buru	GP
2005	3	2	-6.527	129.933	7.1	202	Ambon, Darwin, Sumba, Sorong	GP
2006	1	27	-4.8	127.8	7.4	33	Ambon, Dili, Darwin, Makassar, Sorong	GP
2006	3	14	-3.7	127.4	6.4	33	Ambon, Buru	GP
2009	10	24	-6.18	130.51	7.2	156	Ambon, Serui, Soroon	GP

Events with a tsunami are highlighted in italics. WM Wichmann catalog, LT Latief catalog, BMG BMG Indonesia catalog; K Sololief catalog

respectively. The number of destructive earthquakes has increased since 1975 most likely because of large increases in population and urbanization and better reporting.

Earthquakes in the record cluster in time and space, which is consistent with a stress contagion effect. While the rate of destructive earthquakes remained the same from 1600 to 2014, the size of destructive earthquakes has largely decreased since 1877. No catastrophic earthquake nor tsunami is recorded in the southern Maluku region since 1899. The Banda Islands have not experienced a tsunami higher than 5 m since 1852, whereas it experienced 3 major tsunamis in roughly the same amount of time previous to 1852. The reoccurrence of major earthquake events, such as those that happened in 1629, 1765, 1852 and 1873, will devastate this region now that it has much more to lose.

2.2 1852 Earthquake

The gigantic earthquake of 1852, and the tsunami it produced, is perhaps the largest historic event of its kind in eastern Indonesia (Table 2; van Vliet 1853), which rivals the 1629 event (Liu and Harris 2013). The main shock of the earthquake took place between 7 a.m. and 8 a.m. on November 26, 1852. Later that day, 9 aftershocks were felt. Aftershocks happened daily for the next 8 days and occasionally in the following months and years. The main shock involved 5 min of violent ground shaking as documented in Banda Neira, Rosengain, Pulu Ai, Ambon, Saparua, Haruku, Buru and Seram. Movement was felt as far as Madura Island and East Java (Fig. 4; Table 2; van Vliet 1853), which is 2000 km away from the Banda Islands where most of the damage occurred. The buildings in Banda Neira (Fig. 1) were leveled during the first shock. Ambon (Fig. 1) was rocked by ENE–WSW directional shaking. On Huruku (Fig. 1), Aborn Church and Fort Zeelandia were cracked as the result of shaking. In Surabaya (Fig. 1), Lake Grati was “set in motion” by a weak NW–SE shock.

Following the earthquake, islands in the Banda Sea were inundated by a tsunami (Fig. 5). The details of arrival times and run-up heights for each island were compiled by van Vliet (1853). The “flood wave”, as it is referred to in the historical account, arrived at Banda Neira within 15–20 min. The account records that, “the bay was quickly filled with water, and then just as quickly emptied, such that for a time it appeared to be nothing but a narrow river.” Depth charts of the day show the bay was at least 4 meters deep. After the sea withdrew, tsunami waves crashed into the islands for over 2 h until three big waves arrived at Zonnegat and Lonthor Sound. These waves achieved 8 m run-up heights at Fort Belgica on Banda Neira (Fig. 5a) and completely inundated the coastal plain of Lonthor. The north coast of Banda Neira and south coast of Lonthor were not inundated. On Pulu Ai, tsunami waves were <1 m high.

Ambon bay, which is 200 km from the Banda Islands, was invaded by “a rising of water, which was followed by a fast out flow” shortly after the quake (Fig. 5b). The first five tsunami waves reached a run-up height of 1.8 m and the process continued for over 6 h. Tsunami waves penetrated the Bay of Saparua four times 1 h after the quake and, “reached a height of 3 m above the highest high water level” and inundated 127 m inland. The tsunami was also noted on Haruku, Nasalaut, Buru and Seram (Fig. 5b; Table 2). The record also states that no tsunami was observed at Surabaya and Labuha. Other notable effects from the earthquake were landslides on Banda Neira, Saparua and southeast Haruku, and the birth of at least three new islands in the Kei archipelago. No magmatic activity was observed throughout Indonesia during the event.

Table 2 Historical observations with assigned Mercalli scales (Wichmann 1918)

Region	Locations	Modified Mercalli intensity	Original historical descriptions
Surabaya	Semarang	II	6.45 a.m. A weak shock. Direction NW–SE. In Semarang, as well as in Pasuruan a weak shock was likewise felt. Danau Klinungan, as known as the Lake of Grati, in the district of Grati, Bureau and Locality of Pasuruan, was set in motion. Finally, a weak shock was observed also in Surmenep/Sumenep on the island of Madura
	Pasuruan	II	
	Lake of Grati	III	
	Sumenep	III	
	Labuha	V	4.30, 7, 10, 10.30 a.m. and 6.30 p.m. Labuha, Island of Bajjan. Each time a strong shock; the most powerful among them occurred on the days from the 25th–28th. The flag pole and the trees swayed to and fro. A flood wave was not seen
Banda Islands	Banda Neira, Lonthor	IX	7.50 a.m. Powerful vertical shocks that, waxing in strength, soon transformed into a motion directed NW–SE, of 5 min duration. Already at the first shock, the majority of the residences on Banda Neira were transformed to a rubble heap, but even those that reminded standing had become uninhabitable due to the numerous cracks. A part of Papenberg, upon which the signal station was located, fell away. All along the beach numerous fissures formed. Similar devastations were caused on Lonthor [Banda Major] as well. Barely had the ground been clam for a quarter of an hour when a flood wave crashed in. The bay was quickly filled with water, and then just as quickly emptied, such that for a time it appeared to be nothing but a narrow river. At 10 o'clock the tides increased in force and Banda Neira and Lonthor were thrice poured upon by breakers that had originated in Zonnegat and in the Lonthor Sound. The reached the hill upon which Fort Belgica is built on Banda Neira, and on Lonthor, the foot of the mountains. The difference between the highest and the lowest water level was 26 ft. Feet (8.16 m). On the north coast of Banda Neira, as well as on the south coast of Lonthor, no disturbances of the sea level were manifested. During the quake, a cannonade-like rumble was heard. In the course of the day, 9 further shocks occurred on Banda Neira, of which the first and the fifth were rather powerful
Rosengain Pulu Ai		IX	On the islands of Rosengain and Pulu Ai, the quake was also forcefully manifest. On the latter, the flood wave reached only a few feet above the usual water level. Gunung Api, which forms an island of the same name, did not show the slightest manifestation of volcanic activity
		IX	
Ambon	Ambon, Hila, Larike	IX	7.30 a.m. Violent, wave-formed quake. Duration 5 min. Direction ENE–WSW. Shortly after there came a rising of the water in the bay, which was followed by a fast out flow. The process repeated some twenty times until 2 o'clock in the afternoon. During the first 5 times, the sea (the low water level) climbed to 1.8 m, a height that exceeded the highest high water level by 20 cm. The earthquake and seaquake were also observed in Hila and Larike, but without causing any damages there

Table 2 continued

Region	Locations	Modified Mercalli intensity	Original historical descriptions
Saparua	Saparua Bay, Tjiau, Hatuana, Porto, Kulor, SiriSori, Boi	VII	7.30 a.m. After the earthquake, a flood wave penetrated into the bay of Saparua four times between 8:30 and 11 a, and reached a height of 3 m above the highest high water level. In the environs of the localities Saparua and Tjiau, it thrust itself 405 rh. Feet (127.11 m) inland Beginning at 11 in the morning and until the late evening hours, the high and low tide motions continued n turns, though in lesser amounts On the northeast side, that of the beach area of Hatuana, as also at Porto on the west coast, at Kulor on the north coast, at the two villages of Siri-Sori that lie on the Bay of Saparua, only a week flood wave was observed. In Boi, located on the same bay, a cannonade-like rumble coming from the SE was heard 7.30 p.m. As a result of the vibrations, the walls of the Church of Aborn and the fort Zeelandia were cracked. A flood wave bear the localities Hulaliu, Oma, and Wasu was perceived; in the last-named village was at the same time a cannonade-like rumble
Haruku	Aborn, Hulaliu, Oma, Wasu	VI	
Nasalaut	Amet, Akoon, Leinitu	VI	On the island of Nusalaut, the earthquake had also been palpable and instances of flooding were noted at Amet, Akoon and Leinitu
Buru		V	From the island of Buru was reported merely the fact that an earthquake accompanied by a flood wave had occurred, but without having caused damages
Ceram	Amabai, Wahai	VII	These phenomena manifest themselves in a violent manner on the island of Ceram, at least at the localities of Amabai and Wahai
Ternate		II	8 am. Two shocks in quick succession
Kei Islands			In the vicinity of the island of Ut (5 35'S, 132 59.5'E), Kei lands. According to statements by the natives, islets had arisen as a result of the quake. It was shown through an investigation undertaken by Leut.a. See OUDRAAT on 15 May 1854 that one was almost circular and had a diameter of 250 m. It consisted of clay and on the surface were found several stones and fragments of rioc ore and Manganerz with iron content As R.D.M. VERBEEK visited the first mentioned island in 1899, its Durchmesser was then no more than circa 50 m. It was at the time high tide, and at low tide rose circa 0.25 m above the sea level

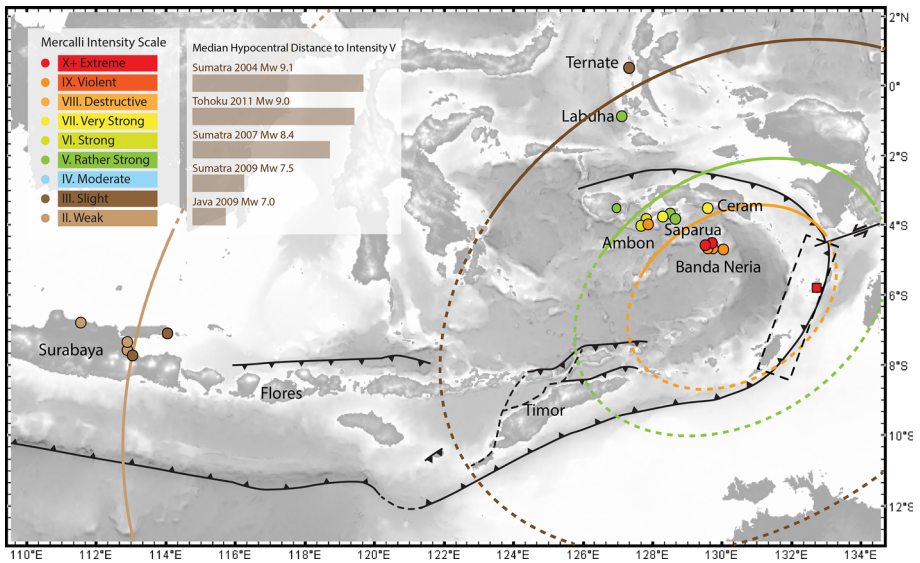


Fig. 4 Reconstructed modified Mercalli scale intensity map of the 1852 earthquake according to descriptions in the Wichmann catalog compiled by van Vliet (1853) and translated into English by Harris and Major (2016). New islands created during the event are represented by red boxes. The dashed rectangle is the most likely rapture zone

2.3 Modified Mercalli intensity map

We constructed a modified Mercalli intensity (MMI) map from descriptions of the 1852 earthquake (van Vliet 1853) with a speculative earthquake epicenter south of the Banda Islands. The MMI contours stretch NE–SW from East Java to Halmahera (Fig. 4). Although land-level changes are common closest to the epicenter of gigantic earthquakes, the new islands that appeared fit the description of mud volcanoes and may have formed at some distance from the epicenter. For example, a $M_w = 7.7$ earthquake in Pakistan on 24 September of 2013 formed new mud volcano islands along the coast nearly 400 km from the epicenter of the event (NASA 2013).

We estimate the distance of the epicenter from various places where the tsunami was observed by using the tsunami propagation equation in the open ocean:

$$V = \sqrt{gD} = d/t$$

where V is velocity of tsunami propagation, g is gravitational force, D is water depth, d is distance between the tsunami source and the location it arrives at, and t is the tsunami arrival time. According to the arrival times of the tsunami noted in the Banda Islands, a reasonable distance to the source of the tsunami is 300–450 km. The most likely source at this distance is the Tanimbar Trough, which marks the subduction boundary between the eastern Banda Arc upper plate and the underthrust Australian passive continental margin.

2.4 Field inspection

We conducted a cursory field investigation of sites both in Banda Neira and Ambon mentioned in historical records that may preserve geological evidence of the 1852

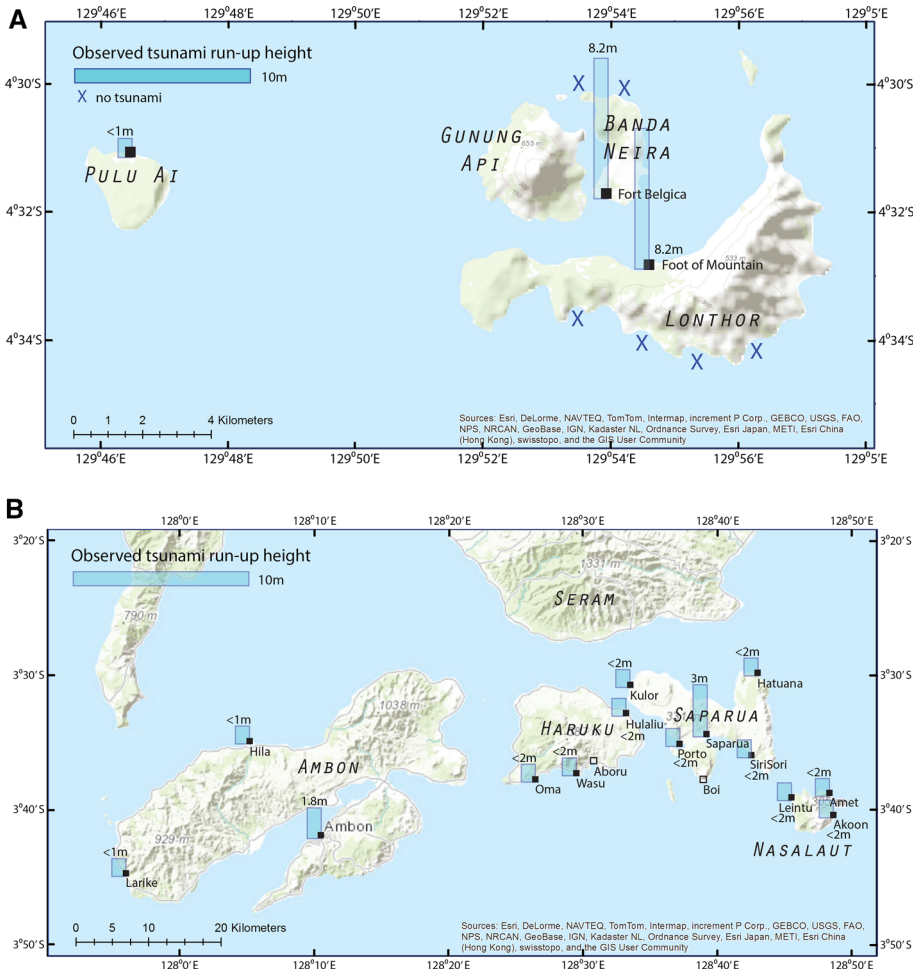


Fig. 5 **a** Map of Banda Islands and Pulu Ai (see Fig. 1). Observed run-up heights in 1852 earthquake according to (van Vliet 1853; Harris and Major 2016) are indicated by blue rectangles. Blue “X” represents no tsunami observation in the area. Locations of virtual tidal gauges (gauge 1, 2 and 5) are indicated by black squares. **b** Map of Uliassera islands (see Fig. 1). Observed run-up heights (blue rectangles) from 1852 tsunami according to (van Vliet 1853; Harris and Major 2016). Other locations mentioned in the catalog with no observed tsunami are shown as open boxes. Locations of virtual tidal gauges (gauge 6–19) are indicated as black squares

earthquake and tsunami. Trenches were excavated near the coasts in both locations. Several candidate tsunami deposits were found with characteristic sedimentary structures (i.e., Monecke et al. 2008) overlying an erosional surfaces covered by shell and human occupation debris. The detailed sedimentology and age relations of these deposits are currently being investigated. However, one trench in Banda Neira (Fig. 6) reoccupied a trench previous excavated by archeologists (Lape 2000). A distinct tsunami deposit around 40 cm thick was located at a nineteenth century stratigraphic level, which is likely from the 1852 tsunami (Fig. 7).



Fig. 6 Photograph of Banda Neira from the top of Banda Api (looking east). The inundation levels of three historical tsunamis that have struck to the island, including the 1852 event, are shown. The 1629 event is reconstructed by Liu and Harris (2013). The trench site location for Fig. 10 is shown

3 Numerical model

We used a series of numerical models to reconstruct the tsunami associated with the 1852 Banda earthquake. Constraints for the models, such as tsunami arrival times, run-up heights and wave-forms, are taken from historic accounts. The models were constructed using GeoClaw from Clawpack (Conservation laws Package), which is designed to solve two-dimensional, depth-averaged, shallow water equations (Berger et al. 2011; LeVeque et al. 2013). It uses high-resolution shock-capturing finite volume methods, allowing adaptive mesh refinement for efficient solutions of large-scale geophysical problems. Clawpack is an open source program provided through the University of Washington and was recognized by the United States National Tsunami Hazard Mitigation Program for hazard-modeling in 2012. GeoClaw is appropriate for modeling large-scale tsunami generated from megathrust earthquakes propagating over a big area. Input parameters are limited to generate fault plane solutions and basic bathymetry data. Adaptive mesh-grid refinement is used for detailed inundation and run-up modeling.

GeoClaw was also used in investigations of slip distributions in the 2011 Tohoku earthquake and the 1952 Kamchatka earthquake, which proved its robustness for modeling large earthquake and tsunami events (MacInnes et al. 2007, 2013).



Fig. 7 Trench into 1852 tsunami deposit in Banda Neira. The upper light colored layer is fine sand near the top of the deposit. Based on archeological studies of the trench (Lape 2000), the stratigraphic interval between the two white bands is likely 1852 tsunami deposit, and the one below it is likely the 1629 tsunami deposit

3.1 Bathymetry/topography

Bathymetric and topographic data in the model are primarily extracted from Digital Elevation Models, ETOPO and Global Multi-Resolution Topography (Amante and Eakins 2009; Ryan et al. 2009). Throughout our modeling, grid resolution ranged between 3'' and 1°. The resolution of initial vertical deformation files is 3'. Grid resolution in the Banda Sea varies between 1° and 30'' during the course of the simulation. A fixed grid is applied at Ambon, the Banda Island and Saparua at a maximum of 3'' for the inundation and runup simulations.

3.2 Fault parameters and vertical seafloor deformation

Fault parameter estimates for reconstructing the 1852 earthquake are taken from fault plane solutions of small instrumental events recorded along the subduction interface in the Tanimbar Trough region. Co-seismic re-bound of the subduction interface at a shallow dip angle (<15°) and shallow depth (<15 km) is a common causes of megathrust earthquakes, such as those in Sumatra (i.e., Zachariassen et al. 1999). Rupture length estimates of the Tanimbar Trough are based on the length of the straightest, uninterrupted segment, which has a maximum length of 540 km, and strikes from 190 to 220°. This segment is truncated to the north by the Tiera Aiduna transcurrent fault and to the south by a sharp bend to the west (Fig. 1). The scaling of the rupture length and width of the simulated earthquake was calculated using empirical relationships compiled by Wells and Coppersmith (1994; Table 3). Models with rupture along two different segments are also used to better fit the curvature of the Tanimbar Trough (Table 4).

Table 3 Wells and Coppersmiths equations (1994)

$$M_w = (5.08 \pm 0.10) + (1.16 \pm 0.07) \times \log(\text{surface rupture length})$$

$$M_w = (4.33 \pm 0.12) + (0.90 \pm 0.05) \times \log(\text{rupture area})$$

Table 4 Fault parameters used in Clawpack modeling

Model	Center of shallowest edge (longitude)	Center of shallowest edge (latitude)	Length (km)	Width (km)	Strike (°)	Dip (°)	Rake (°)	Slip (m)
1	132.92	−5.64	270	80	190	15	90	7
2	132.57	−6.96	270	80	200	15	90	8
3	131.86	−7.75	270	80	220	15	90	12
4	132.81	−6.22	270	80	190	15	90	7
	132.27	−7.31			220			7
5	132.81	−6.22	270	80	190	15	90	7
	132.27	−7.31			220			5
6	132.81	−6.22	270	80	190	15	90	6
	132.27	−7.31			220			8
7	132.94	−5.22	270	80	190	15	90	8
	132.81	−6.22			190			6
8	132.94	−5.22	270	80	190	15	90	6
	132.81	−6.22			190			8
9	132.92	−5.64	540	80	190	15	90	12
	131.86	−7.75			220			12

Poorly constrained shallow water bathymetry for the observation points in the Banda Sea, and no data from near the likely epicenter of the 1852 earthquake, makes it difficult to calculate tsunami wave amplification directly. Generally, tsunami amplification follows the ‘Plafker Rule of Thumb’, which states that the maximum tsunami run-up locally does not exceed twice the height of the deformed seafloor offshore (Synolakis and Okal 2005). However, for the 1852 event, there are no local observations where the ‘rule’ can be applied. The highest waves observed at Banda Neira are 250–350 km away from the likely rupture zone. The orientation of the fault plane is inferred from fault plane solutions of instrumental events likely on the subduction interface. For seafloor deformation, we used a variety of viable fault parameters after Okada (1985; Table 4).

3.3 Amplification factor

We investigated a range of amplification factors, or amplification errors due to low bathymetric data, specifically by testing our model against the 2011 Tohoku earthquake and tsunami. This event has measured run-up heights up to 38.5 m along the northeast coast of Japan. Over 5000 locations were surveyed, which generated the largest tsunami survey database ever for a single event (Mori et al. 2011).

The two-segment rupture model we used for the Tohoku event (Table 5) was constructed using the empirical equation of Wells and Coppersmith (1994). The 5197 on-shore

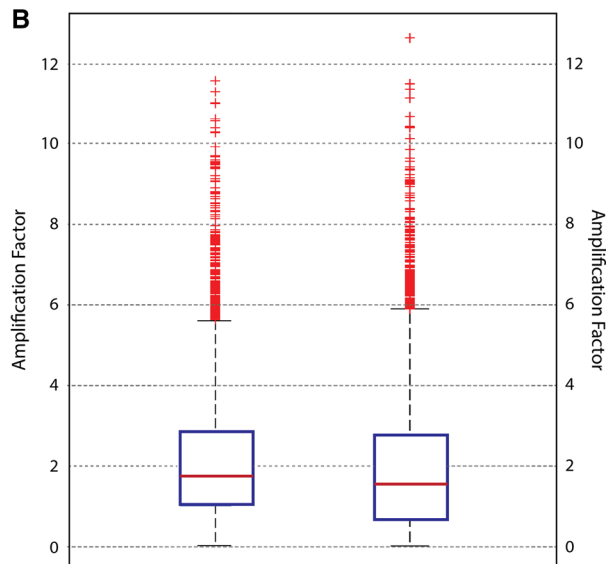
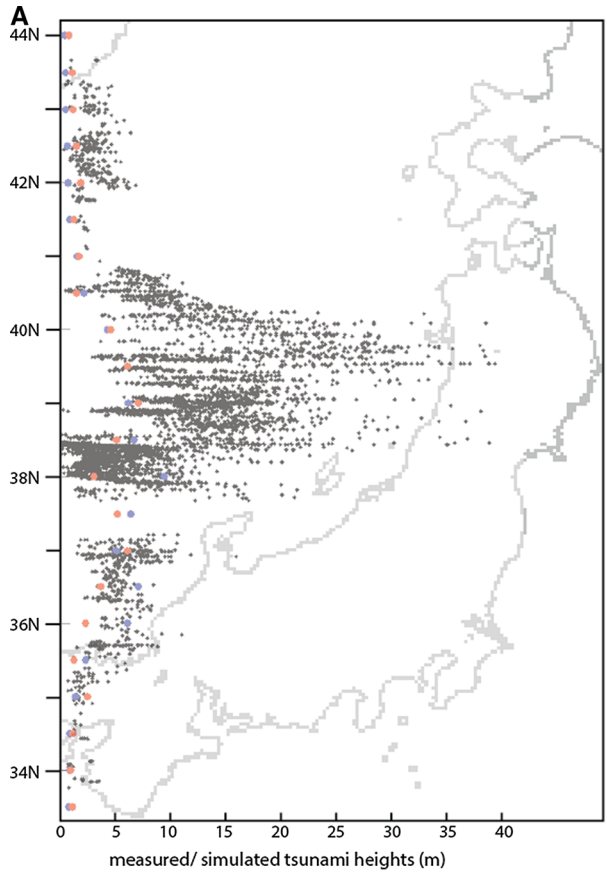
Table 5 Two-fault model for 2011 Tohoku earthquake calculated from Wells and Coppersmiths’ empirical Eq. (1994)

Length (km)	Width (km)	Strike (°)	Dip (°)	Rake (°)	Slip (m)
270	120	190	15	90	30
270	120	210	15	90	30

Table 6 Gauge locations in simulation of 2011 Tohoku earthquake using Clawpack

Latitude of survey locations	Number of survey data	Close-to-shore gauge			Open ocean gauge				
		Latitude	Longitude	Depth (m)	Simulated tsunami height (m)	Latitude	Longitude	Depth (m)	Simulated tsunami height (m)
33.75–34.25	28	34	139.6	-810	0.9	34	141	-4003	0.8
34.25–34.75	11	34.5	139.5	-104	1.1	34.5	141	-5919	0.8
34.75–35.25	31	35	140.05	-77	2.4	35	141.5	-4540	1.3
35.25–35.75	104	35.5	140.5	-20	1.2	35.5	142	-4757	2.2
35.75–36.25	43	36	140.7	-25	2.2	36	142	-3186	6.0
36.25–36.75	125	36.5	140.65	-20	3.6	36.5	142.5	-4377	7.0
36.75–37.25	224	37	141	-40	6.0	37	142.5	-2888	5.0
37.25–37.75	16	37.5	141.2	-63	5.1	37.5	143	-3303	6.3
37.75–38.25	783	38	141	-31	3.0	38	143.5	-4349	9.3
38.25–38.75	1245	38.5	141.7	-154	5.0	38.5	143.5	-2839	6.6
38.75–39.25	916	39	141.9	-122	7.0	39	143.5	-2629	6.1
39.25–39.75	665	39.5	142.2	-286	6.0	39.5	143.5	-2836	6.0
39.75–40.25	347	40	142	-106	4.5	40	143.5	-1780	4.2
40.25–40.75	314	40.5	141.8	-88	1.4	40.5	144	-4246	2.1
40.75–41.25	28	41	141.5	-373	1.6	41	144	-4089	1.5
41.25–41.75	14	41.5	141.55	-101	1.2	41.5	145	-5523	0.8
41.75–42.25	109	42	143.4	-79	1.8	42	146	-5439	0.7
42.25–42.75	126	42.5	143.5	-16	1.4	42.5	147	-5613	0.6
42.75–43.25	48	43	145.15	-38	1.1	43	148	-7196	0.5
43.25–43.75	20	43.5	146.5	-74	1.0	43.5	148.5	-5728	0.4

Fig. 8 a Tsunami measurements from Tohoku Earthquake in 2011 and simulated tsunami heights at close offshore and open ocean settings generated by our model plotted against latitude. Distribution of on shore tsunami measurements (Mori et al. 2011) are represented by *black circles*. Simulated close offshore tsunami heights are represented by *red circles*. Simulated open ocean tsunami heights are represented by *blue circles*. **b** Distribution of amplification factors from the modeling of 2011 Tohoku earthquake. Amplification factors based on simulated close offshore tsunami heights are represented by *box plot on the left*. Amplification factors based on simulated open ocean tsunami heights are represented by *box plot on the right*



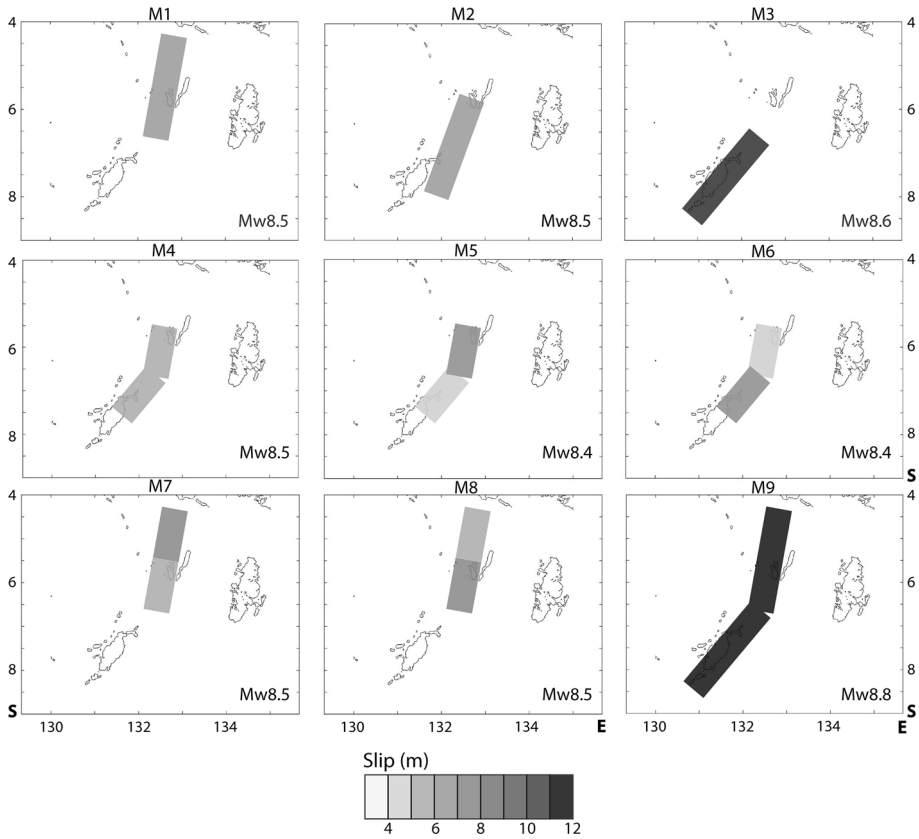


Fig. 9 Various fault rupture models. M1–M9 shows the fault parameters simulated in Model 1–9 respectively (Table 4)

tsunami height measurements are divided into 20 groups, each corresponding to an open ocean virtual gauge and a close-to-shore virtual ocean gauge. Our simulation of the 2011 Tohoku event simulates tsunami heights at these 42 ocean virtual gauges, ranging from 34°N to 44°N (Table 6). Amplification factors are identified as the on-shore tsunami measurements over the corresponding simulated close-to-shore ocean tsunami heights and the on-shore tsunami measurements over the corresponding simulated open ocean tsunami heights (Table 6).

Our simulation of the Tohoku earthquake fails to identify the extreme shoaling at Sendai Plain, Shizugawa, Hirota, Funakoshi and Taro (37°N to 41°N). Minor amplifications in elevations from open ocean waves to close-to-shore waves are shown to the north and south of these areas (Fig. 8a). According to our results, the amplification factors based on close-to-shore virtual ocean gauges have a range from 0.0006 to 12.62 (Fig. 8b). The mean of these estimates is 2.17, while mode and median are 0.60 and 1.75, respectively. The resulting data are highly positively skewed. The same pattern is observed in the amplification factors based on open ocean virtual gauges with mean, mode and median of 2.01, 0.32 and 1.54, respectively. This dataset is again, highly positively skewed (Fig. 8b).

Table 7 Tsunami observations and tidal gauges in 1852 earthquake

Station	Location	Latitude (°S)	Longitude (°E)	Observed run-up heights (m)	Predicted tsunami heights from Model 5 with amplification factor of 2 (m)
1	Banda Neira: Fort Belgica	−4.5320	129.8970	8.2	1.2
2	Lonthor: foot of mountains	−4.5440	129.9080	8.2	1.3
3	Banda Neira: N coast	−4.5066	129.8930	0	0.3
4	Lonthor: S coast	−4.5601	129.8983	0	0.8
5	Pulu Ai	−4.5162	129.7744	<1	0.5
6	Ambon: Ambon City	−3.6900	128.1750	1.8	1.8
7	Ambon: Hila	−3.7550	127.9250	<1	0.3
8	Ambon: Larike	−3.5800	128.0000	<1	0.5
9	Saparua: SiriSori	−3.6065	128.7060	<2	1.4
10	Saparua: Tijau/Saparua Bay	−3.5850	128.6650	3	3.0
11	Saparua: NE: Hatuana	−3.5850	128.6907	<2	1.0
12	Saparua: W: Porto	−3.4943	128.6200	<2	1.5
13	Saparua: N: Kulor	−3.5030	128.5600	<2	2.0
14	Haruku: Hulaliu (NE)	−3.5550	128.6000	<2	3.3
15	Haruku: Oma (S)	−3.6500	128.4420	<2	0.6
16	Haruku: Wasu	−3.6300	128.4930	<2	0.8
17	Nasalaut: Amet (N)	−3.6453	128.8100	<2	1.2
18	Nasalaut: Akoon (SE)	−3.6750	128.8200	<2	0.7
19	Nasalaut: Leinitu (NW)	−3.6550	128.7500	<2	0.7

The scatter in the amplification estimates most likely reflects the high variability in actual bathymetry, which is poorly constrained in the Banda Sea. Local shoaling of waves is beyond the resolution of most bathymetric data sets. The problem is exacerbated by the fact that there are limited observations of the 1852 event compared to the 2011 Tohoku event. Our results are close to the ‘Plafker rule of thumb’ for an amplification factor of two times the slip on the fault. However, this amplification factor of 2 is only applicable to areas with no significant local shoaling.

4 Results

Nine models of various fault parameters were tested (Fig. 9; Table 3). Model 1 and Model 2 simulate a one-segment rupture at the most northern part and middle part of Tanimbar Tough. Model 3 simulates a one-segment rupture at southernmost part of Tanimbar Tough extending to the tip of Timor. Models 1, 2 and 3 are the basis to identify the possible location of maximum slip. Model 4 is a modification of Model 2 with a two-segment rupture including the bend at Tanimbar Islands. Models 5 and 6 use the same rupture area as Model 4 with simple varying slip distributions. Models 7 and 8 are modifications of Model 1, with alternative slip distributions. Model 9 simulates rupture of the entire Tanimbar Tough.

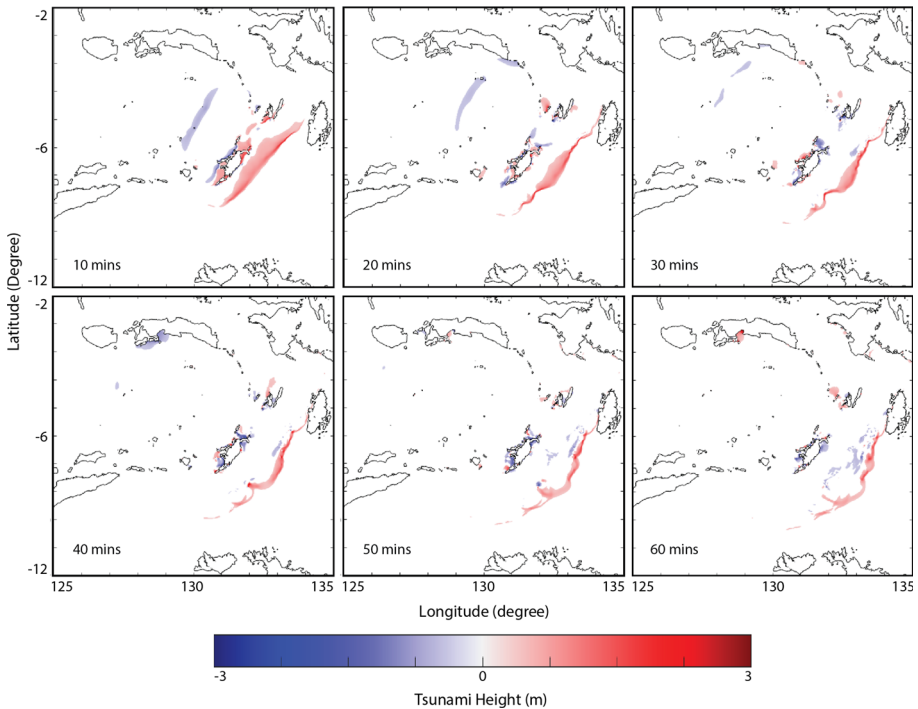


Fig. 10 Snapshots of the first 60 min of tsunami propagation from Model 5 simulation of the 1852 earthquake. Positive tsunami heights are shown in *red*. Negative tsunami heights are shown in *blue*

Using the fault parameters and tsunami amplification factors discussed above yields a minimum moment magnitude of 8.4 if the maximum slip occurs along the north or middle segment of Tanimbar Trough, and 8.6 if the maximum slip occurs along the south segment of Tanimbar Trough (Fig. 9). An amplification factor of 2 is applied at all virtual gauges (Table 7). Simulated tsunami heights are main factor as we determine the best model. However, with potentially extreme shoaling at Banda Neira and Lonthor Island, arrival time of the first wave overrides the importance of simulated tsunami heights at these locations.

Model 5, with maximum slip of 7 m at Kei Islands, produces the best fit between predicted and observed tsunami heights (Table 7). Compared to all nine models, Model 5 generates the highest tsunami run-up at Ambon, Banda Neira and Saparua with the lowest possible moment magnitude. Based on this model, a 1.6 m high tsunami wave arrives at Ambon an hour after the quake and at a 2.7 m wave arrives at Saparua 50 min after the quake (Figs. 10, 11).

The record for Banda Neira does not indicate the height of the initial wave that ‘crashed in’ a quarter of an hour after the earthquake. It does document a dramatic withdrawal after this wave, which is predicted by Model 5. The sea had to have dropped by at least 4 m in order to empty out the bay as reported. It was not until 2 h after the earthquake that the largest waves reaching 8 m arrived at Banda Neira (Wichmann 1918; van Vliet 1853). Tsunami waves that are larger than the first wave to arrive are a common feature of megathrust earthquakes (Atwater et al. 2005). However, existing tsunami models rarely predict these waves (Geist 2010) and presently are mainly reliable for the first few wave

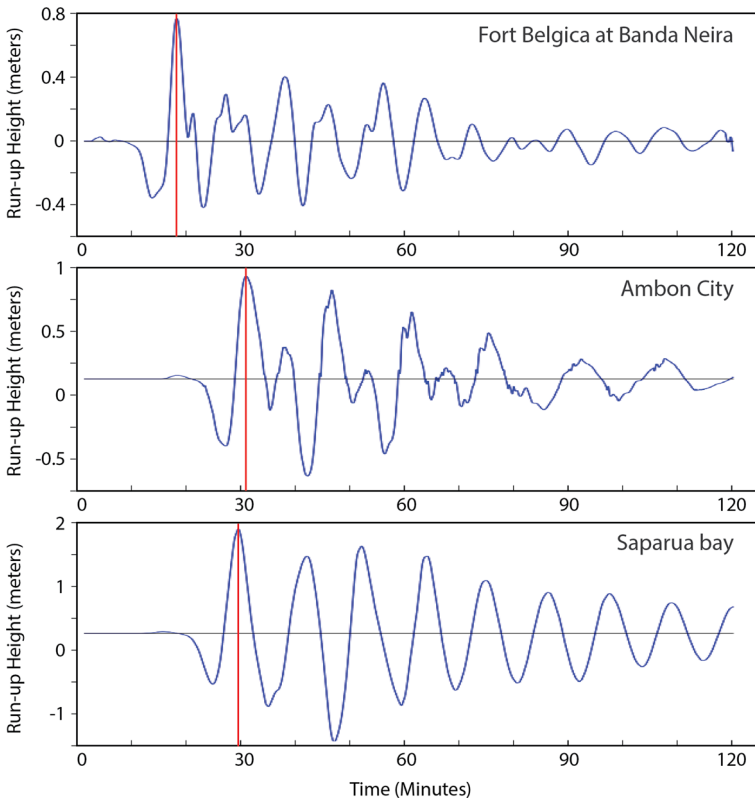


Fig. 11 Computed tide gauge records and tsunami waveform for Banda Neira, Ambon city and Saparua bay stations from Model 5

height and arrival times. Also, the accuracy of run-up height predictions is only as good as the accuracy of the earthquake source parameters used in the models (MacInnes et al. 2013; Arcas and Titov 2006). The lack of instrumental data associated with the 1852 earthquake requires that we use simple rupture scenarios and fault zone parameters. The distribution of slip we use is limited to slip on two fault segments of equal size, which is over simplified compared to slip distributions well constrained by instrumental data.

We varied fault parameters in the same procedure as Liu and Harris (2013) to try to explain the discrepancy between observed and predicted wave heights at Banda Neira, which indicates that the most sensitive parameter is slip. Increasing the fault dip angle from 10 to 15° and the length and width of the rupture zone to the maximum possible values changes the wave height by <10 %.

5 Conclusion

Eastern Indonesia is consistently struck by earthquakes, tsunamis and explosive volcanic eruptions. Records we have compiled provide accounts of destructive geophysical events dating back to 1608. While the rate of earthquakes has remained about the same throughout that time, the size of earthquakes since 1878 in eastern Indonesia has decreased. No

shallow earthquake greater than magnitude 8 or tsunami higher than 5 m has occurred since 1852.

The 1852 earthquake was felt across most of eastern Indonesia and sourced a tsunami that spread throughout the Banda Sea with run-up heights as up to 8 m. Our reconstructions of this event indicate that the tsunami was likely caused by at least an Mw 8.4 earthquake along the Tanimbar Trough. With convergence rates as high as 70–110 mm/a, enough elastic strain energy has already accumulated along the many plate boundary segments in the region to produce another megathrust earthquake and tsunami. Since the 1852 earthquake at least 10–15 m of potential slip has accumulated along the Tanimbar Trough alone, the next 1852-like earthquake will affect a very different Indonesia than in the past, one with 10 times more people that are mostly crowded into coastal urban centers.

Acknowledgments This project was funded in part by National Science Foundation (Grant EAR 0948386) and the Department of Geological Science at Brigham Young University. We express appreciation to Breanyn MacInnes for valuable technical support and advice on the Clawpack software, and for revisions to the manuscript by Summer Rupper and Barry Bickmore. We also appreciate help from the local officials of the Banda Islands and Ambon for facilitating our field investigation.

References

- Amante C, Eakins BW (2009) ETOPO1 1 arc-minute global relief model: procedures, data sources and analysis. In: NOAA technical memorandum NESDIS NGDC-24, 19 pp, March 2009
- Arcas D, Titov V (2006) Sumatra tsunamis; lessons from modeling. *Surv Geophys* 27(6):679–705. doi:10.1007/s10712-006-9012-5
- Atwater BF, Cisternas MV, Bourgeois J, Dudley WC, Hendley II JW, Stauffer PH (2005). Surviving a tsunami—lessons from Chile, Hawaii and Japan. USGS. http://www.tsunamiready.noaa.gov/resources/USGSCircular_1187_rev2005_small.pdf
- Berger MJ, George DL, LeVeque RJ, Mandli KT (2011) The GeoClaw software for depth-averaged flows with adaptive refinement. *Adv Water Resour* 34(9):1195–1206. doi:10.1016/j.advwatres.2011.02.016
- BMKG (2011). Katalog: Gempabumi Signfikan & Merusak 1821–2010, 149 p
- Geist E (2010) The Chilean tsunamis and uncertainty in tsunami modeling. Sound waves, USGS. <http://soundwaves.usgs.gov/2010/04/research2.html>
- Harris RA (1991) Temporal distribution of strain in the active Banda orogen: a reconciliation of rival hypotheses. In: Hall R, Nichols G, Rangin C (eds) Orogenesis in action, *Spec V J Asian Earth Sci* 6(3/4):373–386
- Harris R (2011) The nature of the Banda Arc–continent collision in the Timor Region. In: Arc-continent collision, Springer, Berlin, pp 163–211
- Harris R, Major J (2016) Waves of destruction in the East Indies: the Wichmann catalogue of earthquakes and tsunami in the Indonesian region from 1538 to 1877. In: Cummins PR, Meilano I (eds) Geohazards in Indonesia: earth science for disaster risk reduction. Geological Society, London, Special Publications, p 441. doi:10.1144/SP441.2
- Kelleher J, Sykes L, Oliver J (1973) Possible criteria for predicting earthquake locations and their application to major plate boundaries of the Pacific and the Caribbean. *J Geophys Res* 78(14):2547–2585
- Kreemer C, Holt WF, Goes S, Govers R (2000) Active deformation in eastern Indonesia and the Philippines from GPS and seismic data. *J Geophys Res* 105(B1):663–680
- Lape PV (2000) Political dynamics and religious change in the late pre-colonial Banda Islands. *World Archaeol* 32(1):138–155
- Latief H, Puspito NT, Imamura F (2000) Tsunami catalog and zones in Indonesia. *J Nat Disaster Sci* 22(1):25–43. <http://search.proquest.com/docview/51167018?accountid=4488>
- LeVeque RJ, Berger MJ et al (2013) Clawpack software 4.6.3. www.clawpack.org. Mar 26, 2013
- Liu ZY-C, Harris RA (2013) Discovery of possible mega-thrust earthquake along the Seram Trough from records of 1629 tsunamis in eastern Indonesian region. *Nat Hazard* 72(3):1311–1328
- MacInnes B, Weiss R, Bourgeois J, Pinegina T (2007) Earthquake slip distribution from tsunami deposits and tsunami simulations; the 1952 Kamchatka event. Abstracts with programs—Geological Society of America, 39(6):158. <http://search.proquest.com/docview/50524896?accountid=4488>

- MacInnes BT, Gusman AR, LeVeque RJ, Tanioka Y (2013) Comparison of earthquake source models for the 2011 tohoku event using tsunami simulations and near-field observations. *Bull Seismol Soc Am* 103(2):1256–1274. doi:[10.1785/0120120121](https://doi.org/10.1785/0120120121)
- Minoura K, Imamura F, Sugawara D, Kono Y, Iwashita T (2001) The 869 Jogan tsunami deposit and recurrence interval of large-scale tsunami on the Pacific coast of northeast Japan. *J Nat Disaster Sci* 23(2):83–88
- Monecke K, Finger W, Klarer D, Kong W, McAdoo B, Moore AL, Sudrajat SU (2008) A 1000-year sediment record of tsunami recurrence in northern Sumatra. *Nature*. doi:[10.1038/nature07374](https://doi.org/10.1038/nature07374)
- Mori N, Takahashi T, Yasuda T, Yanagisawa H (2011) Survey of 2011 Tohoku earthquake tsunami inundation and run-up. *Geophys Res Lett* 38(8):0-Citation L00G14. doi:[10.1029/2011GL049210](https://doi.org/10.1029/2011GL049210)
- Newcomb KR, McCann WR (1987) Seismic history and seismotectonics of the sunda arc. *J Geophys Res* 92:421–439. doi:[10.1029/JB092iB01p00421](https://doi.org/10.1029/JB092iB01p00421)
- Nugroho H, Harris R, Lestariya AW, Maruf B (2009) Plate boundary reorganization in the active Banda arc-continent collision: insights from new GPS measurements. *Tectonophysics* 479(1–2):52–65. doi:[10.1016/j.tecto.2009.01.026](https://doi.org/10.1016/j.tecto.2009.01.026)
- NASA Earth Observatory (2013) Earthquake births new island off Pakistan. <http://earthobservatory.nasa.gov/NaturalHazards/view.php?id=82146>
- Okada Y (1985) Surface deformation due to shear and tensile faults in a half-space. *Bull Seismol Soc Am* 75(4):1135–1154. <http://search.proquest.com/docview/51292948?accountid=4488>
- Rangin C, Le Pichon X, Mazzotti S, Pubellier M, Chamot-Rooke N, Aurelio M, Quebral R (1999) Plate convergence measured by GPS across the Sundaland/Philippine sea plate deformed boundary; the Philippines and eastern Indonesia. *Geophys J Int* 139(2):296–316
- Ryan WBF, Carbotte SM, Coplan JO, O'Hara S, Melkonian A, Arko R, Weissen RA, Ferrini V, Goodwillie A, Nitsche F, Bonczkowski J, Zensky R (2009) Global multi-resolution topography synthesis. *Geochem Geophys Geosyst* 10:Q03014. doi:[10.1029/2008GC002332](https://doi.org/10.1029/2008GC002332)
- Soloviev SL, Go CN (1984) A catalogue of tsunamis on the western shore of the Pacific Ocean. Translated by the Canada Institute for Scientific and Technical Information, National Research Council, Ottawa, Canada KIA OS2
- Stein S, Geller RJ, Liu M (2012) Why earthquake hazard maps often fail and what to do about it. *Tectonophysics* 562–563:1–25
- Synolakis CE, Okal EA (2005) 1992–2002; perspective on a decade of post-tsunami surveys. *Adv Nat Technol Hazards Res* 23:1–29. <http://search.proquest.com/docview/51615007?accountid=4488>
- van Vliet L (1853) Prorvo van de beantwoording der vraag: welken invloed moeten de laatste aard. En zeebevingen in de Molukken gencht worden te hebben gehad op de prodnetie der specsrijen. Amsterdam 1853:24–27
- Wells DL, Coppersmith KJ (1994) New empirical relationships among magnitude, rupture length, rupture width, rupture area, and surface displacement. *Bull Seismol Soc Am* 84(4):974–1002
- Wichmann A (1918) Die erdbeben des Indischen Archipels bis zum Jahre 1857 (Earthquakes of the Indian Archipelago Until the Year 1857), in *Afdeling Natuurkunde Nederlandse Verhandelingen*, 20 (1918): 193p
- Yeates R (2012) *Active faults of the world*. Cambridge University Press, Cambridge. ISBN 9780521 190855
- Zachariasen J, Sieh K, Taylor F, Edwards L, Hontoro WS (1999) Submergence and uplift associated with the giant 1833 Sumatran subduction earthquake: evidence from coral microatolls. *J Geophys Res* 104(B1):895–919